Molecular dynamics study of the influence of wall-gas interactions on heat flow in nanochannels

A. J. Markvoort[*] and P. A. J. Hilbers[†]

Department of Biomedical Engineering, Technische Universiteit Eindhoven, Postbus 513, 5600 MB Eindhoven, The Netherlands

S. V. Nedea

Department of Mechanical Engineering, Technische Universiteit Eindhoven, Postbus 513, 5600 MB Eindhoven, The Netherlands

Especially at the nanometer scale interfaces play an important role. The effect of the wettability on the solid-liquid interface has already been studied with molecular dynamics. In this paper we study the dependence of wetting on the solid-gas interface for different density gases and investigate the influence of wetting on the heat transport properties over such an interface using molecular dynamics. Subsequently we show how the flow profile of a gas flowing along a surface also depends on this wettability. These simulations show that wettability increases the conductivity of a solid to a stationary gas and decreases the flow velocity near the interface for a gas flow. These two effects influence the cooling of a solid achieved by a cold gas flowing along its surface in opposite ways. However, we show that a higher wettability has a positive net effect on the cooling, explaining experimental results that showed an increased heat cooling effect of hydrophilic over hydrophobic microchannels.

I. INTRODUCTION

A host of interesting techniques, such as thin film manufacturing, nanotube manufacturing and characterization, the development of materials, and microchannel cooling, demand the prediction of heat transfer characteristics at the nanometer scale [1]. A good example is formed by micro- and nanochannels. These channels can be used to cool mechanical and electrical components in a compact and efficient way. Cooling these devices is essential since most components produce heat when operating. Using a gas or fluid flow through these channels, the devices can be cooled locally where the power is produced. This becomes more and more important as these components become smaller and smaller and produce relatively more power [2]. In this respect, the transport properties of gases at the gas-solid interface play a very important role, and are studied with a host of different experimental and theoretical techniques [3].

Large systems can be described using a continuum approach. However, when the system size decreases or when one focuses on the interface, the continuum approach starts to fail. Much effort has been put into extending macroscopic analyses to microscopic conditions in time and space. For example, the validity of the continuum approach has been identified with the validity of the Navier-Stokes equations [4]. This requires the Knudsen number (Kn=λ/L, where λ is the mean free path of the molecules and L the physical length of the system) to be small compared to unity, with the limit Kn=0.1. When the characteristic size of the device decreases or when the gas is more rarefied, such that Kn>0.1, the

continuum flow model is no longer valid and must be replaced by another model. A possibility is to change the governing equations of the flow model from the Navier-Stokes equations to the Boltzmann equation, which involves the molecular velocities instead of the macroscopic quantities. This integro-differential equation can be solved using a finite element or finite difference method or alternatively using a particle simulation method as the direct simulation Monte Carlo (DSMC) method.

But there are clear limitations to these extrapolations. These are often simplified models, like the DSMC method where particles are represented as hard spheres and boundary conditions are used to represent the gas-solid interface [5,6]. These boundary conditions are a crucial ingredient in continuum fluid mechanical calculations. However, they cannot be derived from the continuum differential equations themselves, and it is often not easy to determine them experimentally.

Close to the interface the continuum approximation does not hold, and detailed knowledge of the influence of the solid-gas interaction is needed. The question remains, however, how large is the influence of the gas-solid interface. An appropriate method to study this is molecular dynamics (MD) [7,8]. MD has long been used in statistical mechanics and chemistry, but can also be used to study microscopic heat transfer phenomena [9]. MD is appropriate because by using this technique the walls can also be modeled explicitly. Various molecular dynamics studies have been performed for very specific gas-solid and fluid-solid interfaces, like, for example, the argon-nickel [10] or the water-platinum [11] interface. Here we perform a systematic molecular dynamics study in order to investigate the influence of the gas-gas and gas-surface interaction parameters on the heat transport over a gas-surface interface, both in the case of a stationary gas and in the case of a gas flow. For this purpose, we studied the behavior of a gas confined between two parallel plates, for gas densities ranging from rare gases to very dense gases and

---

*Electronic address: A.J.Markvoort@tue.nl

†Also at Department of Mathematics and Computer Science, Technische Universiteit Eindhoven, Postbus 513, 5600 MB Eindhoven, The Netherlands.

for various interaction strengths using our parallel molecular dynamics code PUMMA which is based on the code presented in Ref. [12].

The structure of this paper is as follows. In Sec. II the MD simulation technique and the system to be simulated are described. In Sec. III simulation results are shown and discussed subsequently for a system in thermal equilibrium, for a system with a heat flux, and for a microchannel with Poiseuille flow. First, a gas is studied that is confined between two walls of the same temperature. When this system comes to thermal equilibrium, the gas-solid interface can be studied most purely. By systematically changing the parameters of the potential for the gas particle–gas particle interaction, the parameters of the potential for the gas particle–wall particle interaction, or the density, the influence on the behavior at the gas-surface interface can be studied. Subsequently, both walls are assigned a different temperature, allowing for the study of heat flow. By again systematically changing the parameters of the potentials or the density, the influence on the heat flux is studied. Next, also a particle flow is introduced in the gas for which the effect of the interaction parameters on the resulting Poiseuille flow profile is studied. All these effects come together in cooling a solid with a cold gas flow. By letting a cold gas flow between two warm plates, the combined effect of heat transfer over the interface and flow velocity shows which types of interaction yields the best result for cooling the plates. These simulation results are also compared with experimental results. We end in Sec. IV with the conclusions.

II. MODEL

A. Molecular dynamics

Molecular dynamics [7,8] is a computer simulation technique where the time evolution of a set of interacting particles is followed. This is done by numerically solving the equations of motion (Newton's law) of classical multibody systems. Given the positions, masses, and velocities of all particles in the system and the forces on the particles, the motion of all (individual) particles can be followed in time by calculating the (deterministic) particle trajectories.

The force between two particles is governed by the gradient of the potentials between these particles. A commonly used potential is the Lennard-Jones (LJ) potential

$$V_{LJ}(r_{ij}) = 4\epsilon_{ij} \left[\left(\frac{\sigma_{ij}}{r_{ij}} \right)^{12} - \left(\frac{\sigma_{ij}}{r_{ij}} \right)^{6} \right], \quad (1)$$

where ϵ_{ij} is the characteristic energy in the pair potential, σ_{ij} is the collision diameter of the pair, and $r_{ij} = |\vec{x}_j - \vec{x}_i|$ is the scalar distance between particle i and particle j, where $\vec{x}_i$ is the position vector of atom i and $\vec{x}_j$ similarly for particle j. This potential describes the van der Waals interactions and it consists of two parts; a repulsive and an attractive part. For distances smaller than σ_{ij} the resulting force is repulsive, whereas it is attractive for larger distances.

This Lennard-Jones potential is especially appropriate for noble gases, but following [13,14] it can also be used (as a pseudopotential) for metals. Of course, more realistic poten-

tials for metals are available which take into account many-atom interactions, but because LJ interactions capture the essence of all systems and we are not directly interested in one particular metal this potential suffices for our needs.

Formally, in the Lennard-Jones potential all interactions between all nonbonded particles have to be calculated, but since this potential vanishes at larger r_{ij}, only the interactions with particles within a certain cutoff radius $r_{c,ij}$ need to be calculated. Therefore, in our force field one single potential is defined, namely, the truncated shifted Lennard-Jones (TSLJ) potential, which is derived from the standard Lennard-Jones potential as

$$V_{TSLJ}(r_{ij}) = \begin{cases} V_{LJ}(r_{ij}) - V_{LJ}(r_{c,ij}) & \text{if } r_{ij} \leq r_{c,ij}, \\ 0 & \text{if } r_{ij} > r_{c,ij}, \end{cases} \quad (2)$$

which is also shifted upward to avoid discontinuities in the potential.

When a cutoff radius of $r_{c,ij} = 2.5\sigma_{ij}$ is taken into account, the original Lennard-Jones potential is closely resembled. This potential is denoted in the rest of the text as Lennard-Jones.

A second version of this potential is used as well, where the potential is now cut at $r_{c,ij} = 2^{1/6}\sigma_{ij}$, leaving the repulsive part of the potential only, closely resembling hard spheres that are used in other simulation techniques. This potential is denoted further as the Weeks-Chandler-Andersen (WCA) potential.

Our potentials can be thought of in respect to hydrophilic and hydrophobic interactions. Hydrophilic-hydrophilic interactions are described by the LJ potential, where the parameter ϵ_{ij} provides the attraction between the particles. The smaller ϵ_{ij} is, the smaller is the attraction, limiting in the WCA potential, which lacks the attractive part, to describe purely hydrophilic-hydrophobic interactions.

B. Model parameters

Because we are not directly interested in one specific system but in the dependency on the gas-wall interaction, the parameters used in our model are expressed in reduced units. These reduced units, with values typically around 1, improve the numerical stability of the simulations, facilitate error estimation, and can easily be converted to SI units when one wants to model a specific system. The units for length and mass have been chosen as the size and mass of our particles. The unit of energy is chosen such that the parameter ϵ in the potentials, which varies in the different simulations and between wall and gas particles, is around unity. All other reduced units can be derived out of these choices [7,8].

C. System

All simulations that we present to study the gas-solid interface in thermal equilibrium, in the presence of a heat flux, as well as in the presence of a Poiseuille flow, are performed on the same system. The system that we have used for all these studies is shown in Fig. 1. It consists of two walls that are placed in a box of size $80.00 \times 46.89 \times 46.89$, separated from each other in the x direction. These walls consist of
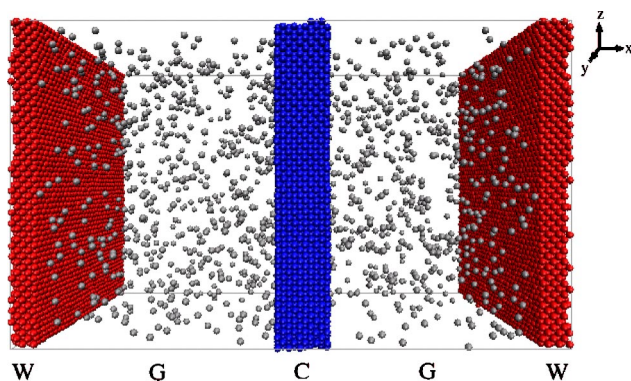
FIG. 1. (Color online) Snapshot of the system simulated: Two fcc walls (W and C) of which the temperature can be controlled separately, and gas in between. The gas density (n_0) in this case equals 0.01. Both the walls and the gas are simulated using molecular dynamics.
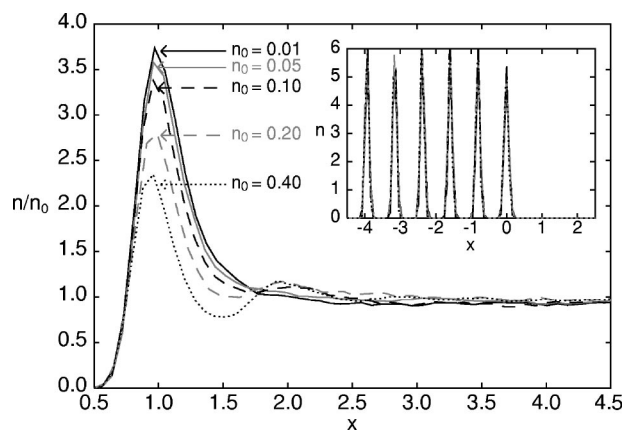

FIG. 2. Profile of the relative density near the wall as a function of the distance to the wall for various gas densities. For both the gas-wall and the gas-gas interactions the LJ potential is used with $\epsilon_{G-G} = \epsilon_{G-S} = 0.5$. The inset shows the density profile of the wall. The last lattice plane of the wall is centered around $x = 0$.

18 000 particles each, where these particles form a face centered cubic (fcc) lattice. We name one wall W and the other C. Because of the use of periodic boundary conditions this represents two infinitely large parallel plates. The space in between the two plates is filled with gas particles (G). Simulations are performed for different gas densities n_0. This density is defined as the number of gas particles divided by the volume available to the gas, i.e., the volume of the simulation box minus the volume of the two walls. The total number of particles in the box ranges from 37 300 for the lowest gas density ($n_0 = 0.01$) to 91 998 for the highest gas density ($n_0 = 0.4$) simulated. The temperature of the two plates can be controlled independently by coupling them to a heat bath, whereas the gas can only heat up or cool down by collisions with these walls.

The walls were formed in a prior simulation. In this simulation 18 000 particles were placed randomly in a simulation box. This system was initially given a high temperature. By cooling this system down the system crystallized. This crystal was placed in a wider box forming one wall. None of the atoms was fixed or restricted in any way such that the walls can in principle move through the simulation box. However, as can be seen, for example, from the clear peaks in the inset of Fig. 2 where the density profile of a wall is given, the walls keep at their position. The mass of a wall is so large compared to the mass of one gas particle that a single collision hardly affects the wall. Multiple collisions are needed, but simultaneously also collisions from the other side of the wall take place. When the system is in equilibrium, the forces on the wall from both sides cancel each other. The walls thus do not need to be restricted in any way. The walls are kept together by the Lennard-Jones interaction between the particles that formed the crystal in the beginning.

The system consists of two types of particles: gas particles (G) and solid (or wall) particles (S). The mass and the size of both particle types are taken equal, namely, the mass of each particle is 1 and the size 1. That the gas particles are in the gas phase whereas the wall particles form a solid is purely controlled by the Lennard-Jones parameter ϵ. For the solid-solid interaction, the LJ potential strength $\epsilon_{S-S} = 6$ is

used whereas for the gas-gas interaction (ϵ_{G-G}) and the gas-solid interaction (ϵ_{G-S}) the LJ potential with values between 0.05 and 0.5 or the WCA potential is used.

The mass and the size of the solid particles could have been chosen differently, but this choice was made to keep the system as simple as possible, though realistic. To show that the values chosen are in realistic ranges, we consider the example of an argon gas and a calcium crystal. In SI units the corresponding LJ parameters are $\epsilon = 0.0104$ eV and $\sigma = 3.40$ Å for Ar and $\epsilon = 0.2152$ eV and $\sigma = 3.60$ Å for Ca. Converting these parameters to our reduced units yields $\epsilon = 6.0$, $\sigma = 1.0$, and $m = 1.0$ for the crystal and $\epsilon = 0.048$, $\sigma = 0.944$, and $m = 0.997$ for the gas.

Every simulation consists of two parts. In the first part the system is run until equilibrium is reached. From the second part, the macroscopic quantities like density, temperature, flow velocity, and heat flux are obtained. The number of iterations differs per simulation as a lower density gas needs more time to come to equilibrium. In order to keep the number of iterations needed for the lowest gas densities tractable we used the following procedure. We start with the highest concentration simulations, where the average gas density (n_0) is 0.40. A configuration from this simulation is taken when it has come to equilibrium and half of the gas particles are removed to obtain an initial configuration for gas density 0.20. This is repeated until the lowest density ($n_0 = 0.01$) is reached. The initial configurations obtained in this way are already closer to equilibrium than randomly generated configurations, but still sufficient iterations were used to let the system come to equilibrium for every concentration. The simulations at the lowest densities, for example, consist of 5 000 000 iterations, taking approximately 200 h on 8 CPU's of our AMD Athlon 1800+ Beowulf cluster.

III. SIMULATION RESULTS

A. Density oscillations near interface

We start by considering the behavior of the gas particles near the wall. The wall influences the nearby gas particles.

As a result the gas density near the wall can deviate from the density in the middle of the channel (the bulk density). These deviations are studied both as a function of the bulk density and as a function of the gas-wall and gas-gas interaction since this behavior at the gas-wall interface is the basis for understanding heat conduction and flow that are studied later.

In order to study the gas particles at the interface most purely the system is studied in thermodynamic equilibrium. Both walls and the gas have temperature $T=1$ and the total momentum of the system is zero. In this case, all four gas-surface interfaces in our system are all identical. Therefore we concentrate our attention on one of them, namely, the interface at the left in Fig. 1. First the influence of the gas density is studied and subsequently the influence of the gas-gas and the gas-wall interaction strengths.

1. Density dependence

The influence of the bulk density on the density near the wall is shown in Fig. 2. In this figure density profiles are shown for gas densities ranging from $n_0=0.01$ to 0.4, where these profiles are all normalized with n_0 to make them comparable. In the inset also the density profile of the wall is shown. From this inset it can be seen that the origin of the coordinate system has been chosen such that the last lattice plane of the wall is centered around $x=0$. The Lennard-Jones parameters used for these simulation both for the gas-gas interaction $\epsilon_{G\text{-}G}$ and for the gas-wall interaction $\epsilon_{G\text{-}S}$ equal 0.5. For all gas densities, the normalized density is slightly lower than unity in the bulk as a result of an increase in the density near the walls. This effect of an increased density near the wall is referred to as wetting of the surface. Particles sticking to the wall are entropically unfavorable, but energetically it is much more favorable for a particle to be near the wall, because there it has more near neighbors and thus more negative energy contributions than in the gas phase. Because this effect is the highest for a low density gas a higher peak in the relative density near the wall is visible for a low density gas than for a high density gas. For a high density gas the interface can also be saturated, resulting in a second layer which is visible as a second peak for the dense gases around $x=2$.

2. Interaction dependence

Apart from the bulk density, the density deviations also depend on the gas-gas and gas-wall interactions. In Fig. 3(a) the density profiles are shown first for the case of a relatively low gas density ($n_0=0.05$) when $\epsilon_{G\text{-}G}$ and $\epsilon_{G\text{-}S}$ are varied simultaneously. Important aspects in this figure are the differences in the heights of the peaks for different interaction parameters and the area in vicinity to the wall. For the WCA potential the first particles are at a larger distance from the wall compared to the LJ potential; we refer to this as the depletion layer for the WCA potential. The differences in peak height can be explained because the larger the interaction parameter of the interaction of gas particles with the wall particles the larger the energetic gain for particles to be close to the wall.

In Fig. 3(b), the density profiles are shown for the case of a relatively high gas density ($n_0=0.4$). Also here the deple-
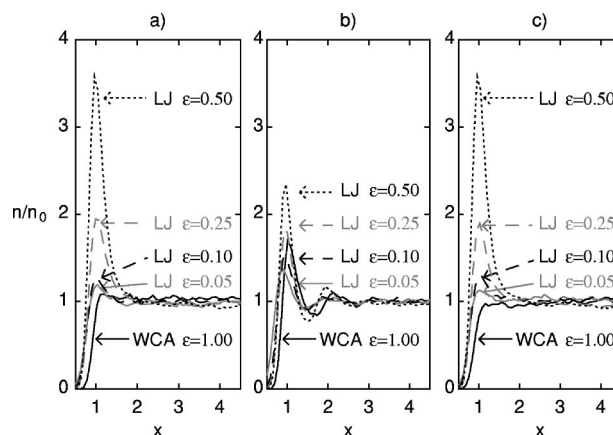

FIG. 3. Density profiles. (a) Density profiles for a low density gas ($n_0=0.05$) for different interaction parameters $\epsilon_{G\text{-}G}=\epsilon_{G\text{-}S}$. (b) The same, but now for a dense gas ($n_0=0.4$). (c) Density profiles for a low density gas ($n_0=0.05$) for different gas-surface interaction parameters $\epsilon_{G\text{-}S}$, but with constant gas-gas interaction (LJ $\epsilon_{G\text{-}G}=0.5$).

tion layer for the WCA interaction potential is visible, although being somewhat smaller. A larger difference is formed by the heights of the density peaks. For the strongest attractive interactions the peaks for $n_0=0.4$ are smaller than for $n_0=0.05$, for which two reasons exist. In the first place, the surface is already much more covered in the case of a high density and in the second place, the bulk particles in a high density gas have already many more close neighbors such that the energetic advantage of being near the wall is relatively smaller than for a rare gas. For the weakest attractive interactions it is the other way around. Here the peaks for $n_0=0.4$ are higher than for $n_0=0.05$. A remarkable difference is that for the high density gas even the WCA potential has a peak in the density near the wall. This can be explained as that the peak in the density is the result not only from the attractive force from the wall, but also from "pushing" by the bulk gas atoms.

Finally, Fig. 3(c) shows the effect of only varying the gas-wall interaction while keeping the gas-gas interaction at 0.5 in case of the low density gas. Comparison with Fig. 3(a) shows hardly any differences, indicating that, for low density gases, the influence of the gas-gas interaction parameter is negligible compared to the gas-surface interaction parameter.

For low gas densities the density peak at the interface thus depends on the attractive part of the gas-wall interaction potential. The higher the interaction of the gas with the wall, the higher the gas density near the wall. An explanation for this is that in the presence of an attraction between the gas and the wall, some gas particles stick to the wall for some time. To study this the time (Δt) spent by a particle per collision with a wall is measured. A way to measure this time is to measure the time that a particle in a low density gas spends within an interface region which is defined as a slice of width 2 from the center of the last surface lattice plane. The particles in a low density gas with a density of $n_0=0.01$ have a mean free path of about 22, which is much larger than the width of the interface region. As a result, the chance that a particle collides with another gas particle in
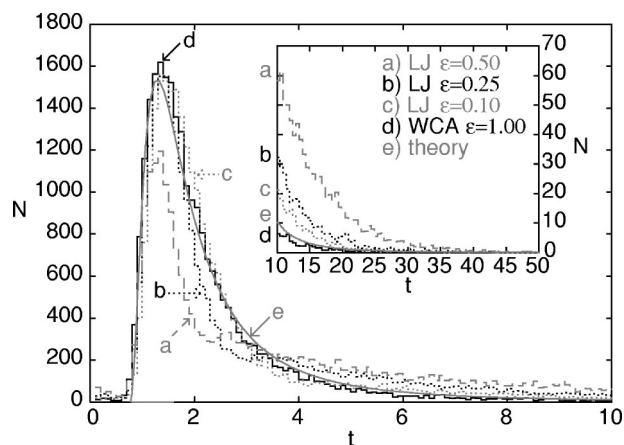
FIG. 4. Histograms of the time spent per particle per collision with a wall within the interface region for different gas-wall interaction parameters. The inset zooms in at the tails.
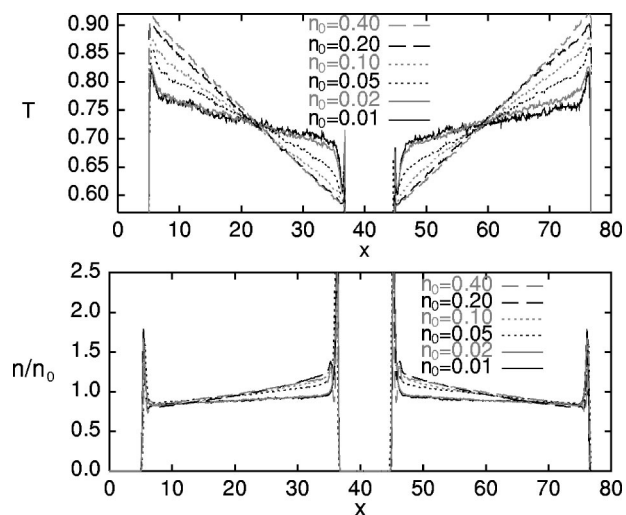

FIG. 5. Temperature and density profiles of the gas for different gas densities when one wall has a temperature $T=1.0$ whereas the other wall is kept at $T=0.5$.

this interface region is small such that the time spent in the interface region by a particle equals the distance to be traveled in the interface region in the x direction divided by its velocity in the x direction plus the time spent at the interface. In Fig. 4 histograms of this time (Δt) spent by a particle per collision with a wall within the interface region are given for different gas-wall interaction parameters for a gas density $n_0=0.01$ and gas and wall temperature $T=1$. In the same figure also the theoretically expected time distribution is given for the case of reflective walls. In this theoretically expected time distribution an additional collision time of 0.15 is added to account for the time needed to flip the velocity at the interface. The velocity cannot just flip from negative to positive, instead, the particle should decelerate and again accelerate in the opposite direction resulting in the extra time. For the WCA interaction, in case there is no attracting force of the wall, the distribution is close to this theoretical result. In the case of an attractive gas-surface interaction, high velocity particles are hardly affected, but slower particles are caught by the wall. As a result, the peak decreases for average collision times as these particles are trapped for a while and are thus visible for even higher residence times as can be seen clearly in the inset in the same figure.

Summarizing, density peaks at the interface can have two distinct roots. In the first place they are the result of gas particles sticking to the wall because of the energetic gain. For high gas densities they are also the result of other gas particles pushing from only one side, the bulk side. Next we will study how this wetting influences heat conduction.

B. Heat flux dependence on wettability

To study the heat conduction a temperature difference between the two plates is implied. One wall, the warm wall W, is kept at temperature $T=1.0$ whereas the other wall, the cold wall C, is kept at temperature $T=0.5$. As a result, the gas in between the two plates shows a temperature gradient. The influence of the gas density as well as the influence of the gas-gas and gas-wall interactions on this temperature gradient are studied.

1. Density dependence

For $\epsilon_{G\text{-}G}=\epsilon_{G\text{-}S}=0.25$, the temperature and normalized density profiles for different gas densities are shown in Fig. 5. From the figure it is clear that when the average gas density is higher, a higher temperature gradient is present in the gas. Furthermore, for high densities the temperature profile is linear, whereas for low densities it is linear in the bulk and different near the interfaces. These increased gradients in the temperature near the interfaces coincide with the increased density near these interfaces.

Xue *et al.* [15,16] studied the effect of ordering near the walls for the solid-liquid interface, also using MD. They concluded from their simulations that the layering of the liquid near the interface does not enhance the thermal transport. Our results for high density gases which limit to the liquid phase match with this conclusion. However, for lower density gases, an enhanced thermal transport is clearly visible from the increased temperature gradients in Fig. 5, an effect that is outlined in the next section.

Another property that can be derived from our simulations is the heat current. The heat current vector is given by [17]

$$\vec{q} = \frac{d}{dt}\sum_i \vec{x}_i E_i, \tag{3}$$

where the summation is over all the particles in the system, and $\vec{x}_i$ and E_i are the position vector and energy of particle i, respectively. For a pair potential, such as the potentials that we use, Eq. (3) can be recast as

$$\vec{q} = \sum_i \vec{v}_i E_i + \frac{1}{2}\sum_{i,j} (\vec{F}_{ij} \cdot \vec{v}_i)\vec{r}_{ij}, \tag{4}$$

where $\vec{v}$ is the velocity vector of a particle, and $\vec{r}_{ij}$ and $\vec{F}_{ij}$ are the interparticle separation and force on particle i by particle j, respectively. Because of the geometry of our system we are here interested in the x component of this vector, i.e., q_x. This heat flux in the x direction as a function of the gas
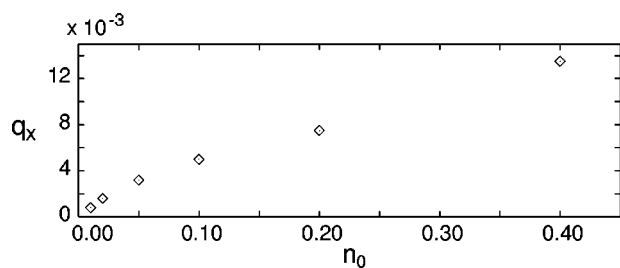
FIG. 6. The heat flux q_x for different gas densities for $\epsilon_{G\text{-}G}$ $=\epsilon_{G\text{-}S}=0.25$.

density is shown in Fig. 6. This heat flux can also be calculated by measuring the energy that is added and removed by the heat bath that is used to keep the walls at their constant temperature. This energy divided by the simulation time and twice the area in the yz direction of the simulation box yields the same numbers. An increase in the density clearly results in an increase in the heat flux.

2. Interaction dependence

As shown in the previous section, for a gas density n_0 $=0.01$ large temperature jumps occur near the walls. From Fig. 7 it can be seen that the exact shape of these jumps depends on the gas-gas interaction and the gas-wall interaction. In this figure the density and temperature profiles are given for three different values for $\epsilon_{G\text{-}G}$ and $\epsilon_{G\text{-}S}$. In the top part of the figure it can be seen that the temperature gradient increases with increasing attraction in the potential. In the lower set of figures, just the interface region is shown. This figure shows that the width of the temperature jump overlaps with the width of the density peak near the wall. This increased density near the wall comes from wetting, as we have seen in Sec. III A 2.

As a result of particles sticking to the wall, their velocity is adapted much more to the wall temperature than for particles that only make a single collision with the wall. This can be seen in Table I, where the number of particles (No.)

TABLE I. The difference in average temperature of particles moving in the direction from the cold to the warm wall ($C \rightarrow W$) versus particles moving in the opposite direction ($W \rightarrow C$) depends on the gas interaction parameters.

Potential	$C \rightarrow W$		$W \rightarrow C$	
	No.	T_{av}	No.	T_{av}
WCA	294	0.71	292	0.75
LJ 0.10	287	0.71	274	0.75
LJ 0.25	281	0.68	261	0.77
LJ 0.50	225	0.62	204	0.80

and their average temperature (T_{av}) for particles moving from the warm to the cold wall and for particles moving from the cold wall to the warm wall have been given for the bulk gas (thus excluding the interface region) of the left compartment. The higher the attraction with the wall the fewer particles in the bulk and at the same time the higher the difference in temperature between gas particles moving to the left and particles moving to the right.

As can be seen from Fig. 8 this also influences the heat flux. In this figure the heat flux is given for different combinations of interaction parameters for the same gas density ($n_0=0.01$). From this figure it is clear that the differences in heat flux for different gas-gas interactions are minimal, whereas the differences in heat flux for different gas-wall interactions are considerable. We thus notice again that the relevant parameter is the gas-wall interaction strength, whereas the gas-gas interaction is of much less influence on the resulting heat flux. An increased gas-wall attraction thus results in an increased ordering at the interface and an increased heat flux, grounding our conclusion from the previous section that for gases, contrary to liquids, the layering near the interface enhances thermal transport.
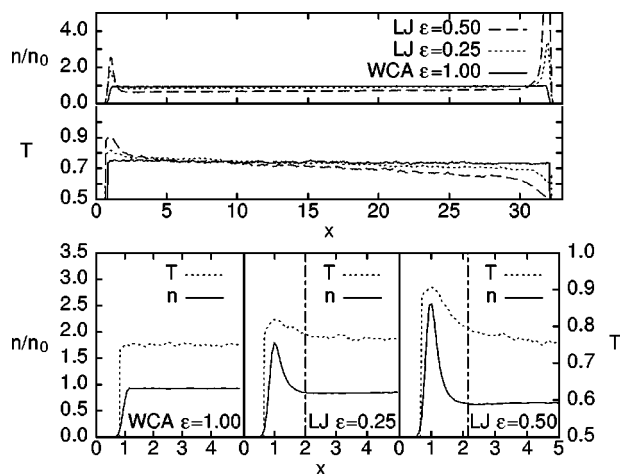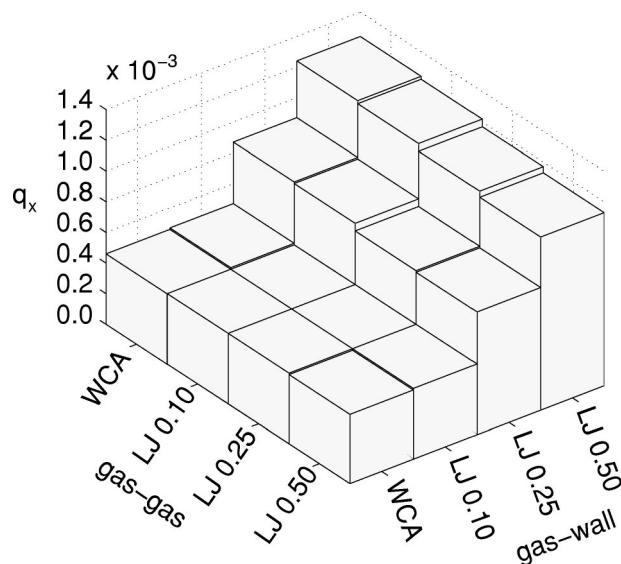

FIG. 7. (Top) Density and temperature profiles of the gas for different gas interaction parameters. (Bottom) Same profiles zoomed in at the interface region.

FIG. 8. The heat flux q_x for different parameters for the gas-gas as well as the gas-wall interaction for a low gas density $n_0=0.01$.
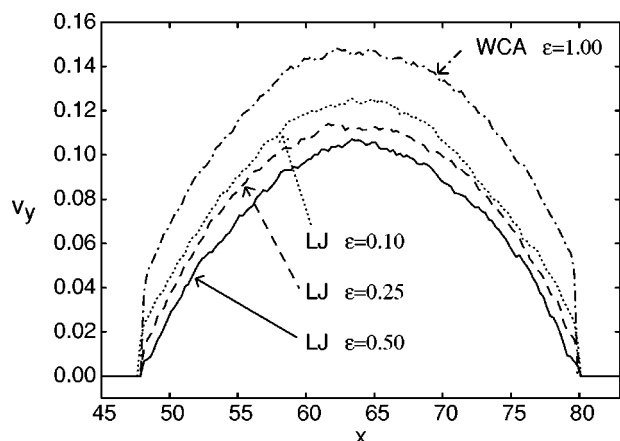
FIG. 9. Flow velocity distributions in the channels for different gas-wall interaction parameters.

C. Gas flow dependence on wettability

The wettability influences not only heat transport. As shown by Cieplak *et al.* [18,19] and Nagayama and Cheng [20], also the flow profile of a liquid near a solid-liquid interface depends on the interface wettability.

A Poiseuille flow can be induced in the model in different ways. The first method is a gravitational flow. This is achieved by applying an additional force to all gas particles. A second method, the one that we use in this paper, is a pressure driven flow. This is created by applying the additional force only to the gas particles at the inlet of the channel. In order to generate a flow in the positive y direction, i.e., from the back to the front in Fig. 1, an additional force in the y direction is applied to all gas particles with a y coordinate between zero and 3, i.e., in a small slice at the back of the figure.

Because of this additional force the gas starts to flow. Because the wall particles are not restricted in position and there is friction between the gas and the wall, the walls start to move also. There are again several ways to prevent this. One solution that is often applied is to add additional harmonic forces to all wall particles to keep them close to their original position. However, since we do not want to add any additional forces to restrict the walls we apply a different method. We repeatedly remove the linear momentum that is transferred from the gas to the wall because of the friction. By resetting the total linear momentum of the wall particles to zero every ten iterations, when this total linear momentum is still negligible, the walls remain at their place without having to constrain the particles within the walls.

The friction between the wall and the gas increases with the flow velocity and when the total frictional force equals the additional force on the gas particles an equilibrium flow is reached, resulting in a velocity profile that is quite Poiseuille in appearance. The resulting flow profiles for different gas-wall interactions are shown in Fig. 9 for a gas density $n_0=0.4$ and $\epsilon_{G\text{-}G}=0.25$. All four velocity profiles have the same shape as expected since the gas-gas interaction is the same. The difference between the four profiles is the velocity of the gas at the interface. Since the walls are stationary this velocity at the interface is the slip. As we have seen, in case

of a strongly attractive force between the gas and the wall particles, gas particles stick to the wall resulting in such a large friction that the flow velocity at the interface is zero, i.e., no slip. However, the lower the gas-wall attractive interaction, the smaller the friction and thus the larger the slip. For the case of the purely repulsive gas-wall interaction the extra depletion layer between the wall and the gas results in an even lower friction and thus an even larger slip.

D. Cooling warm walls with a cold fluid

As we have shown, the wettability influences the heat transfer over the interface as well as the flow velocity at the interface. And both effects are influenced in an opposite fashion: an increased wettability results in an increased heat transfer and at the same time in a decreased flow velocity. When cooling warm walls with a cold gas flow, both these effects play a role.

In order to study this heat transfer from warm walls to a cold fluid, the temperature of the fluid has to be reset when it crosses the periodic boundary. This can be achieved by rescaling the velocity of every particle that crosses the periodic boundary in the flow direction. The temperature is defined as the deviations in the velocities from the local mean flow velocity. The rescaling is thus performed by first subtracting the local mean velocity corresponding to the x position of the particle, subsequently rescaling the velocity to the desired temperature and finally again adding the local mean flow velocity that was removed in the beginning.

The results for a gas inflow temperature 0.9 and walls at temperature 1.0 are shown in Fig. 10 for two different gas-wall interaction parameters. On the left side the profiles are shown for the LJ potential with $\epsilon_{G\text{-}S}=0.25$, whereas the right hand side part is for the WCA potential with $\epsilon_{G\text{-}S}=1.0$. For the gas-gas interaction in both cases the LJ potential is used with $\epsilon_{G\text{-}G}=0.25$.

The profiles at the top show the density distribution. Because of the attractive interaction between the gas and the wall particles density peaks appear again in case of the LJ interaction, whereas there is again a dip in the density near the walls in case of the repulsive WCA interaction. The profiles in the middle show the flow velocities in the channels. It is clearly visible that the flow for the WCA potential is again higher than for the LJ potential. The attraction with the wall causes friction resulting in hardly any slip near the walls. However, in case of the repulsive interaction, a large slip at the walls is present. But the attractive interaction also enables more heat transfer between the wall and the gas, thus resulting in a higher temperature of the gas in case of an attractive interaction than in case of repulsive interaction as can be seen from the profiles at the bottom of the figure.

In order to keep the walls at their constant temperature, as much energy has to be added from the heat bath to the walls as is removed from the walls by the gas. The net effect of the wettability on the cooling can thus be studied by measuring this energy that is added to the walls by the heat bath. For the simulations described above, the heat that is carried away equals 50 units of energy per unit of time for the WCA gas-wall interaction versus 52 units of energy per unit of
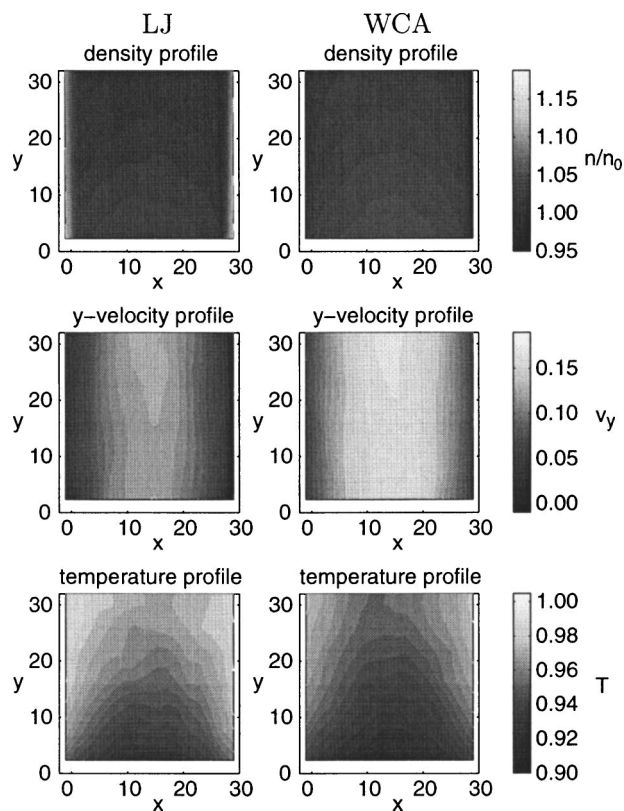
FIG. 10. (Color online) Density, flow velocity, and temperature distributions in the channels for a gas at temperature $T=0.9$ flowing along the walls at temperature $T=1.0$ for two different sets of interaction parameters: (left) LJ interaction between gas and wall particles, (right) WCA interaction between gas and wall particles, whereas the gas-gas interaction is the same in both cases (LJ $\epsilon_{G\text{-}G}$ $=0.25$).

time for the LJ gas-wall interaction. The cooling is thus slightly better for the LJ gas-wall interaction. However, when the forces to generate the flow for the case of the LJ gas-wall interaction are increased with 45% such that the mean flow velocity equals that of the WCA case, the amount of heat that is carried away increases to 135 units of energy per unit of time. Thus, at the expense of an increasing pressure drop much more heat can be carried away.

Thus, although the flow is smaller, the amount of heat that can be removed is larger in case of attractive walls because of the better heat transfer over the interface. This explains the results of experiments of convective heat transfer in silicon microchannels with different surface conditions, i.e., a microchannel with hydrophilic walls versus a microchannel with hydrophobic walls [21].

IV. CONCLUSION

Two potentials were used to describe the gas-wall interaction; the Lennard-Jones potential with different interaction strengths and the WCA potential for a purely repulsive interaction. The most remarkable difference in the resulting density profiles at the interfaces is that hard sphere gases result in a depletion layer compared to LJ gases.

In case of an attractive gas-surface interaction an increased density near the wall is visible for all gas densities. For a purely repulsive gas-surface interaction this increase is only visible for high gas densities. Thus, for high densities the gas is not only attracted by the wall but also pushed against the wall by the other gas particles in the bulk.

From varying the gas-surface interaction only on one side and both the gas-surface and the gas-gas interactions on the other, it is clear that the gas-gas interaction is not as important as the gas-surface interaction for the behavior at the interface.

Whereas the increased layering at the solid-liquid interface for higher solid-liquid binding strength seems to have no effect on the thermal conductivity [15], the solid-gas binding strength seems to have an effect on the solid-gas thermal conductivity.

Hard sphere (WCA) interaction results in specular walls whereas strong attractive (LJ) interaction results in thermal walls. The amount to which a wall behaves like a thermal wall depends on the gas-wall interaction strength.

In the case of flow, also the flow profile depends on the gas-wall interaction strength. The weaker the interaction, the larger the slip at the interface. Thus in case of a cold flow along a warm wall there are two opposite effects. The heat transfer from the wall to the gas is enhanced for high attractive interaction whereas this causes the gas to flow slower. But the net result is that more heat can be transferred in case of an attractive interaction than in the case of a purely repulsive interaction. This explains the results from Wu and Cheng [21] who concluded that the Nusselt number and apparent friction constant of trapezoidal microchannels having strong hydrophilic surfaces (thermal oxide surfaces) are larger than those having weak hydrophilic surfaces (silicon surface). This suggests that convective heat transfer can be enhanced by increasing the surface hydrophilic capability at the expense of increasing pressure drop.

Also note that one should be very careful with using simplified methods to study phenomena where interfaces play a key role, since the behavior at these interfaces determine ultimately the behavior of the whole system. Hybrid methods (see, e.g., [22,23]) could play here an important role.

[1] A. Majumdar, Microscale Thermophys. Eng. **4**, 77 (2000).

[2] R. Schmidt and B. Notohardjono, IBM J. Res. Dev. **46**, 739 (2002).

[3] G. Somorjai, Surf. Sci. **335**, 10 (1995).

[4] G. A. Bird, *Molecular Gas Dynamics and the Direct Simulations of Gas Flows* (Clarendon Press, Oxford, 1994).

[5] A. Frezzotti, Eur. J. Mech. B/Fluids **18**, 103 (1999).

[6] A. Frezzotti, Phys. Fluids **9**, 1329 (1997).

[7] *Computer Simulation of Liquids*, edited by M. Allen and D. Tildesley (Oxford University Press, Oxford, 1987).

[8] D. Frenkel and B. Smit, *Understanding Molecular Dynamics* (Academic Press, San Diego, 2002).

[9] D. Poulikakos, S. Arcidiacono, and S. Maruyama, Microscale Thermophys. Eng. **7**, 181 (2003).

[10] V. Chirita, B. Pailthorpe, and R. Collins, J. Phys. D **26**, 133 (1993).

[11] T. Kimura and S. Maruyama, in Proceedings of the 12th International Heat Transfer Conference, 2002 (unpublished), pp. 537–542.

[12] K. Esselink, B. Smit, and P. Hilbers, J. Comput. Phys. **106**, 101 (1993).

[13] T. Halicioglu and G. Pound, Phys. Status Solidi A **30**, 619 (1975).

[14] P. Guan, D. R. Mckenzie, and B. A. Pailthorpe, J. Phys.: Condens. Matter **8**, 8753 (1996).

[15] L. Xue, P. Keblinski, S. Phillpot, S. Choi, and J. Eastman, Int. J. Heat Mass Transfer **47**, 4277 (2004).

[16] J. Eastman, S. Phillpot, S. Choi, and P. Keblinski, Annu. Rev. Mater. Res. **34**, 219 (2004).

[17] A. McGaughey and M. Kaviany, Int. J. Heat Mass Transfer **47**, 1783 (2004).

[18] M. Cieplak, J. Koplik, and J. Banavar, Physica A **287**, 153 (2000).

[19] M. Cieplak, J. Koplik, and J. Banavar, Phys. Rev. Lett. **86**, 803 (2001).

[20] G. Nagayama and P. Cheng, Int. J. Heat Mass Transfer **47**, 501 (2004).

[21] H. Wu and P. Cheng, Int. J. Heat Mass Transfer **46**, 2547 (2003).

[22] A. Frijns, S. Nedea, A. Markvoort, A. van Steenhoven, and P. Hilbers, *Lecture Notes in Computational Science*, Proceedings of the 4th International Conference, Krakow, Poland, 2004, Vol. 3039 (Springer, Berlin, 2004), p. 661.

[23] S. Nedea, A. Frijns, A. van Steenhoven, A. Markvoort, and P. Hilbers, Phys. Rev. E (unpublished).